



Published in final edited form as:

Int J Cancer. 2018 September 01; 143(5): 1162–1175. doi:10.1002/ijc.31400.

Alternative splice variants of DCLK1 mark cancer stem cells, promote self-renewal and drug-resistance, and can be targeted to inhibit tumorigenesis in kidney cancer

Yang Ge¹, Nathaniel Weygant^{2,3}, Dongfeng Qu^{2,3,4,5}, Randal May^{2,3,5}, William L. Berry⁶, Jiannan Yao¹, Parthasarathy Chandrakesan^{2,3,4}, Wei Zheng⁷, Lichao Zhao⁷, Karena L. Zhao⁷, Michael Drake⁸, Kenneth J. Vega⁹, Michael S. Bronze², James J. Tomasek⁶, Guangyu An¹, Courtney W. Houchen^{2,3,4,5}

¹Department of Oncology, Beijing Chao-Yang Hospital, Capital Medical University, Beijing, China

²Department of Medicine, The University of Oklahoma Health Sciences Center, Oklahoma City, OK

³COARE Biotechnology Inc., Oklahoma City, OK

⁴The Peggy and Charles Stephenson Cancer Center, Oklahoma City, OK

⁵United States Department of Veterans Affairs Medical Center, Oklahoma City, OK

⁶Department of Cell Biology, The University of Oklahoma Health Sciences Center, Oklahoma City, OK

⁷Department of Pathology, The University of Oklahoma Health Sciences Center, Oklahoma City, OK

⁸Coagulation Biology Laboratory, Oklahoma Medical Research Foundation, Oklahoma City, OK

⁹Department of Medicine, National Jewish Health, Denver, CO

Abstract

Renal cell carcinoma (RCC) is a common and devastating disease characterized by a hypoxic microenvironment, epithelial-mesenchymal transition and potent resistance to therapy evidencing the presence of cancer stem cells (CSCs). Various CSC markers have been studied in RCC, but overall there is limited data on their role and most markers studied have been relatively

Correspondence to: Courtney W. Houchen, MD, 920 Stanton L. Young Blvd, WP. 1345, Oklahoma City, OK 73104, Tel.: (405)271-2175, Fax: (405)271-5450, courtney-houchen@ouhsc.edu; or Guangyu An, PhD, 8 Gongren Tiyuchang Nanlu Road, Chaoyang Dist., Beijing 100020, China, Tel.: 86-010-85231407, Fax: 86-010-85231570, anguangyu@hotmail.com. Y.G. and N.W. contributed equally to this work

Author Contributions

Y.G., N.W., G.A. and C.W.H. proposed the original concept. Y.G. and N.W. reviewed the literature, designed the study and wrote the manuscript. Y.G., N.W., D.Q., R.M. and J.Y. performed the experiments, analyzed the data and prepared the figures. N.W., D.Q., R.M. and M.D. designed, generated, purified and characterized the CBT-15 monoclonal antibody. D.Q. and W.L.B. generated cDNA plasmids and lentivirus to create essential materials for the study. W.Z., L.Z., K.Z. and N.W. performed pathologic examination, characterization and/or quantification of the stained tissue. C.W.H., G.A., J.J.T., K.J.V., M.S.B. and P.C. reviewed the manuscript and provided expertise and administrative and material support. All authors read and approved the final manuscript.

Conflict of interest: C.W.H. is a cofounder of and majority owner of COARE Biotechnology Inc. N.W., D.Q. and R.M. have minority ownership of COARE Biotechnology Inc. All other authors declare no conflict of interest.

Additional Supporting Information may be found in the online version of this article.

nonspecific. Doublecortin-like kinase 1 (DCLK1) is a validated CSC marker in the gastrointestinal tract and evidence for an equivalent role in other cancers is accumulating. We used bioinformatics, immunohistochemistry, flow cytometry, spheroid self-renewal and chemoresistance assays in combination with overexpression and siRNA-knockdown to study the stem cell-supportive role of DCLK1 alternative splice variants (DCLK1 ASVs) in RCC. To target tumor cells expressing DCLK1 ASVs directly, we developed a novel monoclonal antibody (CBT-15) and delivered it systemically to RCC tumor xenografts. DCLK1 ASVs were overexpressed, enriched together with CSC markers and predictive of overall and recurrence-free survival in RCC patients. *In vitro*, DCLK1 ASVs were able to directly stimulate essential molecular and functional characteristics of renal CSCs including expression of aldehyde dehydrogenase, self-renewal and resistance to FDA-approved receptor tyrosine kinase and mTOR inhibitors, while targeted downregulation of DCLK1 reversed these characteristics. Finally, targeting DCLK1 ASV-positive cells with the novel CBT-15 monoclonal antibody blocked RCC tumorigenesis *in vivo*. These findings establish DCLK1 as a CSC marker with implications for therapy, disease progression and survival in RCC and demonstrate the therapeutic value of DCLK1-targeted monoclonal antibodies against renal CSCs.

Keywords

DCLK1; cancer stem cell; renal cancer; resistance; monoclonal antibody therapy

Introduction

Renal cell carcinoma (RCC) is a common cancer,¹ and 48% of patients present with regional or distant spread. RCC is characterized by a 12.3% 5-year survival rate for metastatic disease, and a 40% recurrence rate in localized disease, even after surgical resection.¹⁻³ Moreover, RCC is intractable because of resistance to chemotherapies and radiation. Currently, targeted therapies including immunotherapy, receptor tyrosine kinase inhibitors and mTOR inhibitors are the main treatments for RCC.⁴ However, none of these therapies result in durable responses, and novel therapies are necessary to improve prognoses.

VHL mutations and silencing are the most common event in RCC development. Because of this loss, hypoxia-inducible factors such as HIF1A can escape proteasomal degradation and drive hypoxic conditions supporting angiogenesis.⁵ Although these processes provide a basis for RCC initiation, other processes also provide support for RCC's significant intratumor heterogeneity⁶ and notable resistance to radiation and drug therapies.⁷ Among these is epithelial-mesenchymal transition (EMT)^{8,9} which may, in combination with a hypoxic microenvironment and HIF1A activation,¹⁰ provide a supportive environment for tumor stem cells (TSCs). Together these characteristics may contribute to the prevalent metastatic presentation and tendency for recurrence and drug-resistance in human RCC,^{5,6,9} and form a basis for targeting TSCs and related targets to improve outcomes.

Doublecortin-like kinase 1 (DCLK1) is a validated gastrointestinal TSC marker correlated to initiation, EMT, and progression.¹¹⁻¹³ Moreover, tumor-specific expression and extracellular isoform localization make DCLK1 viable for targeted therapies.¹⁴⁻¹⁶ In RCC, DCLK1 is

epigenetically dysregulated and overexpressed on the gene and protein level. Furthermore, DCLK1 downregulation impairs invasion and spheroid formation in RCC.¹⁶ Here, we demonstrate that specific DCLK1 isoforms are associated with renal TSC markers, and able to predict survival and recurrence in RCC. Moreover, overexpressing these isoforms modulates resistance to FDA-approved therapies. Finally, treatment with a novel isoform-specific DCLK1 monoclonal antibody (CBT-15) impairs tumor growth *in vivo*. These findings support a potential role for DCLK1 in renal TSCs¹⁶ which may account for its value as a prognostic marker and therapeutic target in this disease.

Materials and Methods

Construction of human DCLK1 Isoform 2 cDNA sequence

DCLK1 Isoform 2 constructs are not commercially available so we utilized a 364 bp gBlock synthetic DNA containing human DCLK1 Isoform 1 sequence shared with Isoform 2, and DCLK1 isoform 2C-terminal sequence (NCBI RefSeq: XM_005266592.2). The vector containing DCLK1 Isoform 1 and the gBlock were digested with EcoRI and ScaI, followed by gel purification and ligation. The ligated cDNA was confirmed by automatic sequencing. DCLK1 Isoform 2 vector was then constructed into lentivirus as described previously.¹³ RCC cell line Caki-2 was infected with lentivirus to overexpress DCLK1 Isoform 2/long- α (Caki2-dsRed-DCLK1) or red fluorescent protein (RFP) cDNA as control (Caki2-dsRed) and selected to 100% expression.

Cell culture

Caki-2 and ACHN human RCC cells were obtained from ATCC and Sigma-Aldrich, respectively, where they were tested and authenticated via morphology, karyotyping and PCR to rule out interspecies and intraspecies contamination. Cells were cultured in RPMI medium containing 10% fetal bovine serum (FBS) at 37°C and 5% CO₂.

siRNA-mediated knockdown of DCLK1

Caki-2 10⁵ or ACHN cells were seeded into 6 cm dishes and allowed to attach overnight. Lipofectamine 3000 was complexed with 25 nM of commercially validated siRNA targeting human DCLK1 coding region (siDCLK; sc-45618) or 25 nM scrambled sequence (siSCR) not matching any known genes. After 72 hr of transfection, RNA and protein were collected to confirm knockdown.

Quantitative real-time RT-PCR

Total RNA was isolated using Tri-Reagent. Reverse transcription was performed using SuperScript II and random hexanucleotide primers. cDNA was used to perform real-time PCR on an iCycler IQ5 (BioRad). To detect specific transcripts, gene-specific primers (Supporting Information Table 1) and JumpStart™ Taq DNA polymerase were used. β -actin was used to normalize the threshold value and assess quantitative changes.

Western blotting

Protein concentration was determined by BCA assay. Forty microgram of protein lysates were size separated on a 4–20% SDS polyacrylamide gel and transferred onto a PVDF membrane. The membrane was blocked in 1% casein for 30 min and probed with primary antibody α -DCLK1 (ab31704), HIF-1 α (ab2185), Vimentin (SC-7557), ALDH1A1 (ab52492), β -Actin (ab8226) overnight at 4°C. The membrane was washed with TBST and probed with secondary antibody for 30 min at RT. Proteins were detected using a LICOR Odyssey Imager.

Proliferation/drug resistance assay

Cells (5,000/well) were seeded into a 96-well plate in quadruplicate, and cultured with sorafenib, sunitinib, everolimus, temsirolimus with DMSO as a vehicle at varying concentrations. 48 or 72 hr after incubation, 10 μ L of MTT was added to each well and incubated at 37°C for 4 hr. When crystalline precipitate became visible, 50 μ L DMSO containing 266 mM NH₄OH was added to the wells for dissolution. Absorbance was measured using a microplate reader and results were normalized to vehicle-treated wells.

3D spheroid assay

Reduced growth-factor matrigel was mixed with cell suspensions containing RPMI medium (volume 1:1). Hundred microliter of mixture was pipetted into 96-well plates at 50 cells/well. After matrigel solidification, 50 μ L RPMI medium with 10% FBS was added to each well. The plates were then incubated at 37°C under 5% CO₂. The media was refreshed weekly and wells monitored for spheroids. For drug response, after 72 hr drug treatment, the cells were trypsinized and seeded following the protocol above. The cells were allowed to form spheroids for 10–15 days, defined by >15 cells and plates were washed with PBS and fixed with formalin. Spheroids were counted manually.

Angiogenesis coculture assays

HUVEC cells (ATCC) were expanded to two passages and seeded into 24-well plates containing growth-factor reduced matrigel at 3.33×10^4 cells per well. Standard EGM was used to stimulate tube formation and cells were treated with vehicle (DMSO) or sunitinib (200 nM) alone or below transwells seeded with ACHN cells pretransfected with siSCR or siDCLK1 for 48 hr. DCLK1 knockdown was confirmed by Western blot. After 24 hr, images from each well were taken with a microscope at 10x magnification including five images from the circumference and five images from the center. Tube formation was manually measured using ImageJ. Total tubule length, mean tubule length and number of branches were calculated. For additional representative images of direct coculture, this assay was repeated in a 6-well dish with cell number appropriately adjusted and final images were taken after two weeks at 4x magnification.

Immunohistochemical automated cell counting

The tissue microarray was scanned using a digital pathology scanner and saved in SVS format. The SVS file was loaded into QuPath (OSX) and the sections dearrayed. After dearray, tissue was detected with the *simple tissue detection* function. DAB-positive cells

were detected using *positive cell detection* and negative cells were detected by hematoxylin. Segmentation accuracy was confirmed visually. Automated counts and percentages were used for analysis.

Flow cytometry

To assess cell cycle, cells were trypsinized, centrifuged at 4°C, washed with cold PBS and fixed in 70% ethanol on ice for >2 hr. Following fixation, cells were washed and incubated with propidium iodide (50 µg/mL) and RNase A. To analyze DCLK1 expression, cells were trypsinized, centrifuged, washed and then 5 µL activated ALDEFUOR and 5 µL anti-DCLK1 antibody conjugated with APC-Cy7 were added and allowed to incubate for 60 min at 37°C. Following incubation, cells were washed with ALDEFUOR buffer. Data was collected on FACS Calibur and analyzed in ModFit LT or Flowing Software. To analyze ALDH expression, cells were resuspended in ALDEFUOR assay buffer containing ALDH substrate, BAA (Bodipy-aminoacetaldehyde) (50 mg dry reagent), with or without 5 mL of diethylaminobenzaldehyde as a negative control. After 1 hr of incubation at 37°C, data was collected. For DCLK1 extracellular-domain based sorting, cells were trypsinized and washed as described above. After washing, cells were incubated with anti-DCLK1 antibody for 60 min on ice and sorted using BD Biosciences FACS Aria III. Sorted cells were kept on ice and seeded into ECM.

Monoclonal antibody

DCLK1-targeted therapeutic monoclonal antibody (CBT-15 mAB), an analogue of a previously reported DCLK1 mAB,¹⁷ and isotype control mAB were supplied in PBS (COARE). DCLK1 affinity was confirmed by ELISA and Western Blot. ELISA for CBT-15 was performed with 5% BSA blocking and commercial DCLK1 purified protein (Origene).

In vitro ADCC assay

ACHN cells were seeded into a 96-well plates at 5×10^4 cells/well and allowed to attach overnight at 37°C. CBT-15 mAB or isotype control were added to the ACHN wells at 100 µg/mL in quadruplicate and incubated at 37°C for 72 hr. After mAB treatment, the media was replaced and 1.25×10^5 primary human PBMC cells (ATCC) were coincubated with the ACHN cells for 72 hr. Finally, CaspaseGlo® 3/7 activity (Promega) assay was performed according to the manufacturer's protocol.

Xenograft tumor study

ACHN cells (5×10^5) were injected subcutaneously into male athymic nude mice flanks and allowed to grow until the tumor reached an average of 100 mm³. Once this volume was reached, CBT-15 or isotype mAB was delivered intraperitoneally at 25 mg/kg biweekly and tumor volume measurements were taken every other day. Tumor volume was calculated using the formula: volume = 0.5LW². Mice were killed by CO₂ asphyxiation and tumors excised, weighed and measured. All studies were performed in accordance with standards set forth by the OUHSC Institutional Animal Care and Use Committee.

Immunohistochemistry

Immunohistochemistry was performed as previously described¹⁶ for PD-L1 and DCLK1 using a microarray (US Biomax, KD2085). Staining results were quantified by clinical pathologists blinded to the sample identity. A composite score was calculated by multiplying the assessed value for stain intensity (0–4) and percent tissue involved (0–4).

Datasets, visualization and statistical analyses

RNA-seq results were obtained from TCGA Pan-Cancer datasets (xenabrowser.net). Basic statistical analyses were performed using R v3.2, SPSS Statistics 19, Graphpad Prism 7.0 and Microsoft Excel. One-way ANOVA and the Student's *t* test were used to determine significance. For nonparametric comparisons the Wilcoxon test was used. Kaplan–Meier and Cox regression analyses for patient survival were performed and visualized using the *survival* and *survminer* packages in R and Graphpad Prism 7.0, and correlation plots were prepared with the *corrplot* package in R. KEGG pathway analysis was performed using the gene set analysis toolkit (webgestalt.org).¹⁸ Homology models were predicted using the SPARKS^X Fold Recognition web server (sparks-lab.org).¹⁹ For all analyses $p < 0.05$ was considered to be statistically significant.

Results

Alternative splice variants of DCLK1 are overexpressed in RCC patient tumors

We previously reported that DCLK1 is overexpressed in RCC compared to adjacent normal tissue.¹⁶ To further evaluate DCLK1's expression in kidney cancers, we analyzed The Cancer Genome Atlas (TCGA) PAN-CANCER RNA-seq dataset. DCLK1 was most overexpressed in clear cell renal carcinoma followed by papillary renal carcinoma. Conversely, it was downregulated in chromophobe kidney cancers (Fig. 1a). To investigate pathways enriched in DCLK1+ tumors, we compared transcriptomes between high and low DCLK1– expressing clear cell renal carcinoma (RCC) tumors using the nonparametric Wilcoxon test and performed KEGG enrichment. From ten enriched pathways, six were immunity-related, suggesting that DCLK1 may play a role in the immune response to RCC (Supporting Information Table I).

We evaluated DCLK1 protein expression by immunohistochemical (IHC) staining using a tissue microarray. The results confirmed our TCGA findings demonstrating DCLK1 overexpression in clear cell, papillary and sarcomatoid kidney cancers (Fig. 1b). Qualitative analysis of IHC of normal tissue shows that DCLK1 is primarily cytoplasmic and present in both the smooth muscle and endothelial blood vessel cells in proximity to glomeruli. Moreover, it is expressed with moderate and occasionally strong intensity in some renal epithelial tubules (Fig. 1c). This finding may be significant as the proximal tubule is thought to be the cell of origin for ccRCCs,²⁰ and vasculature supports progression in renal malignancy. Comparatively, normal tissue adjacent to malignancy shows little DCLK1 expression in blood vessels and tubules, and decreased expression overall. Instead, DCLK1 is frequently nuclear and most often found in individual cells within the tubular epithelium, suggesting that DCLK1-based signaling may be altered in disrupted tissue (Supporting Information Fig. 1a). In sarcomatoid and papillary RCC, DCLK1 is expressed in tumor

cells with weak to strong intensity. Both highly specific and diffuse staining may be present in these tumor types. In sarcomatoid RCC, DCLK1 expression appears to be associated with spindle cell morphology and is primarily cytoplasmic, but membrane and nuclear staining may also be present. DCLK1 is also expressed diffusely in RCC cells with rhabdoid morphology and prominent megacytosis. In papillary RCC, DCLK1 may be strongly expressed in the cytoplasm and membrane of papule tumor cells and moderately but specifically expressed in enlarged, dysplastic adjacent tubules (Supporting Information Figs. 1b–1d). In clear cell RCC, DCLK1 expression varies from sparse staining in early stage tumors to prominent, intense staining of large tumor regions in more advanced stages (Fig. 1c; enlarged image panels: Supporting Information Figs. 2a and 2b). However, we observed both early stage tumors with high intensity DCLK1 and later stage tumors with low intensity DCLK1. Overall, expression is usually found in tumor cells, tumor-associated vasculature or both—and most ccRCC and associated cells express DCLK1 in the cytoplasm, membrane or both—though nuclear staining may also be present (Supporting Information Figs. 2a and 2b). To quantify DCLK1+ cells per tumor section, automated segmentation analysis was performed with QuPath²¹ (Supporting Information Fig. 3). Settings were adjusted for conservative quantification to increase confidence by excluding cells with overly diffuse or low intensity DCLK1, which could lead to false positives. In normal tissue, approximately 2% of cells were positive on average compared to 0.3–0.5% in sarcomatoid and papillary RCCs. Clear cell RCC had the highest number of positive cells with an average of 3% (Fig. 1d), and consistent with our visual intensity scoring and qualitative assessment showing increased DCLK1 expression with progression, Stage I ccRCC had 1.24% DCLK1+ cells compared to 4.29% for Stages II and III (Supporting Information Fig. 5a). Altogether, these findings show that DCLK1 is expressed in common RCC subtypes and its specific localization in tumor epithelia and vasculature may be desirable for targeted therapies. Moreover, DCLK1+ cells are often sparsely distributed especially in early stage RCC, and mitotic events giving the impression of self-renewal or rarely asymmetric division are sometimes associated with them (Supporting Information Fig. 2a, Upper Left Panel). Both characteristics are suggestive of potential TSCs, although conclusions should not be drawn from this initial IHC characterization. Further analyses of DCLK1 distribution in RCC patient tumors at different time points or perhaps from orthotopic models may be informative in understanding the significance of these findings.

Because of varying functions and localizations of DCLK1's isoforms^{13,16,22} it is necessary to maintain awareness of their profile. DCLK1 alternative-splicing resulting from an exon skip leads to two additional variants with lengthened C-terminals.²³ To assess these in RCC, we used the isoform-specific RNA-seq data generated during the TCGA PAN-CANCER project. Isoform 1 (DCLK1-short- α ; UniProtKB: O15075–2; ENST00000255448.8), Isoform 2 (DCLK1-long- α ; UniProtKB: O15075–1; ENST00000360631.7) and Isoform 4 (DCLK1-long- β ; UniProtKB: O15075–4; ENST00000379893.5) are overexpressed in RCC (Fig. 1e). However, Isoforms 2 and 4 (alternative splice variants) show a greater differential compared to Isoform 1. It is notable that the antibody used to perform the immunohistochemistry described is also specific to the “long” products of DCLK1 alternative splicing (i.e., Isoforms 2 and 4 which have lengthened C-terminals). These findings suggest that DCLK1 has a favorable expression profile for therapy. Moreover,

DCLK1 demonstrates isoform-specific overexpression that may be key for biomarker development.

DCLK1-long isoforms are prognostic factors in clear cell renal cancer

DCLK1 is prognostic in colorectal, head and neck, lung and other cancers.^{24,25} To determine if DCLK1 is prognostic in RCC we performed Cox regression and Kaplan–Meier survival analyses. Tumor DCLK1 predicts recurrence in RCC ($p < 0.005$) with low level DCLK1 (<25th percentile) prognosticating an approximately 2.5% five-year recurrence rate compared to approximately 20% and >35% for mid and high expression, respectively. Moreover, this rate is stable for up to 11 years whereas tumors expressing mid or high levels of DCLK1 are associated with a 38–43% recurrence rate (Fig. 2a). Cox regression analyses revealed that these differences were associated with DCLK1 Isoforms 2 (long- α) and 4 (long- β) ($p < 0.001$ and $p < 0.02$, respectively), but not Isoform 1/short- α (Supporting Information Table II). However, despite significant differences in recurrence-free survival (RFS) associated with total DCLK1 gene expression, Cox regression analysis of overall survival demonstrated no significant difference (Supporting Information Table II). Given these somewhat confounding results, and our previous hypothesis that DCLK1 expression may be more significant in early cancer before the DCLK1+ cell's progeny dilute its signal,²⁵ we assessed clinical subgroups. In this context, DCLK1 Isoforms 2 or 4 were able to predict reduced OS in patients with low-grade disease ($p < 0.05$). However, DCLK1 Isoform 1 expression predicted the opposite, suggesting that it may have a differing function and be expressed in different cells than Isoforms 2/4 in RCC (Fig. 2b). Using Fisher's exact test, we found a significant inverse relationship between DCLK1 Isoform 1 and stage, tumor size and lymph node status explaining this apparent discrepancy. Moreover, relationships between DCLK1 Isoforms 2/4 and gender and age suggest that these factors should be considered in future studies (Fig. 2c). These findings support further investigation of DCLK1-long isoforms as RCC biomarkers.

RCC tumors expressing high levels of DCLK1-long isoforms are enriched for cancer stem cell markers

DCLK1 has a prominent role in TSCs in the gastrointestinal tract^{12,26,27} and data supports a similar role in other cancers.¹⁶ Although RCC displays TSC characteristics (drug resistance, hypoxic microenvironment, EMT), research into their role has been limited. Aldehyde dehydrogenase (ALDH/ALDH1A1) is the most prominent RCC TSC marker and is linked to tumorigenesis and mortality.²⁸ Additional targets increased in RCC TSCs include CXCR4, which also predicts progression,^{29,30} and CD44.³¹ To gauge DCLK1's potential to mark renal TSCs, we compared ALDH1A1, CXCR4 and CD44 expression levels in tumors expressing high and low levels of DCLK1 isoforms. Tumors expressing DCLK1-long isoforms (Isoforms 2 and 4) were enriched for these markers compared to those expressing low levels (Supporting Information Figs. 4a and 4b). In contrast, tumors expressing high levels of DCLK1-short- α (Isoform 1) demonstrated no statistical difference (Supporting Information Fig. 4c). Another measure of stemness in RCC, CD44/24 ratio, also demonstrated enrichment in tumors expressing DCLK1-long isoforms, but no difference in tumors expressing DCLK1-short- α (Supporting Information Fig. 6a). These findings suggest DCLK1-long isoforms are coexpressed with renal TSC markers. Moreover, they support

differing roles between DCLK1-short and long isoforms in RCC, as well as a molecular basis to explain their prognostic potential (Supporting Information Fig. 4d).

DCLK1-long- α drives molecular and functional stemness in renal cancer cells

To investigate DCLK1-long in RCC we overexpressed DCLK1-long- α (Isoform 2) in Caki-2 cells (Caki-2-dsRed-DCLK1). Overexpression of the DCLK1-dsRed fusion protein was confirmed by western blot, real-time PCR and microscopy (Figs. 3a and 3b). Overexpression of DCLK1-long- α modestly increased cell proliferation, but did not affect the cell cycle (Supporting Information Figs. 6b and 6c). Moreover, overexpression led to increased ALDH1A1 and HIF1A (Figs. 3a and 3b) consistent with our RNA-seq analysis (Supporting Information Fig. 4a). Additionally, we found increased vimentin which is associated with RCC survival,¹⁶ and increased immune checkpoint proteins PD-L1 and CTLA4 which are the targets of novel therapies^{32,33} and a mechanism by which EMT-supported TSCs avoid immune-mediated destruction.^{34–38}

To assess DCLK1-long- α in functional stemness, we compared spheroid formation capacity of Caki-2-dsRed and Caki-2-dsRed-DCLK1 cells. After two weeks, spheroids were fixed, counted and quantified using ImageJ. DCLK1-long- α increased the size and number of spheroids formed (Fig. 3c). Moreover, immunocytochemistry demonstrated strong ALDH1A1 expression in DCLK1-overexpressing spheroids compared to faint ALDH1A1 protein expression in controls (Fig. 3d). These findings suggest that DCLK1-long- α and ALDH1A1 may cooperate in renal TSCs and led us to hypothesize the presence of a double-positive population.

To test the hypothesis that ALDH/DCLK1-long double-positive cells are present in RCC, we performed FACS on unmodified ACHN and Caki-2 cells. Both lines demonstrated a large population of ALDH+ cells (>50%) as measured by Aldefluor reagent and a smaller population of DCLK1-long1 cells (7–18%). However, despite the large percentage of ALDH+ cells, ALDH/DCLK1-long++ cells accounted for only 0.5–1.5% of total cell population consistent with a minority subpopulation, as by chance a 5.5–9.8% double-positive population would be expected ($p < 0.05$) (Fig. 4a). Furthermore, we performed FACS analysis for ALDH on the DCLK1-long- α overexpression cell line (Caki-2-dsRed-DCLK1). ALDH+ cells as measured by Aldefluor reagent were increased in Caki-2-dsRed-DCLK1 cells compared to vector control cells (Fig. 4b). These findings demonstrate that DCLK1 and ALDH are linked at the cellular level and together with the spheroid data support the possibility that they mark a population of renal TSCs.

Extracellular DCLK1-long marks a subpopulation of RCC cells with increased clonogenic capacity

Extracellular markers of TSCs are desirable for targeted therapies. We hypothesized that some of the minority subpopulation of DCLK1+ cells observed in our FACS experiments (Figs. 4a and 4b) might express extracellular DCLK1. To evaluate this hypothesis, we sorted DCLK1+ cells under nonpermeabilizing conditions from the ACHN line by FACS using antibody targeting the extracellular domain of DCLK1 and isotype control to exclude cells with nonspecific staining (Fig. 4c). Following FACS, cells were seeded into extracellular

matrix for 3D colony formation. Following two weeks of growth, ACHN-DCLK1+ cells formed more spheroids (>25%) compared to ACHN-DCLK1- cells (Fig. 4d). This finding demonstrates that extracellular DCLK1-long is present in a population of RCC cells with enhanced clonogenicity and provides evidence that DCLK1 supports RCC functional stemness.¹⁶

DCLK1-long is a source of resistance to receptor tyrosine kinase inhibitors in RCC

Drug resistance is a clinical characteristic of RCC. Moreover, it is a mechanism by which quiescent TSCs maintain viability while the bulk of the tumor is destroyed by chemotherapies targeting rapidly dividing cells preferentially. To determine DCLK1's contribution to this process, we subjected Caki-2-dsRed or Caki-2-dsRed-DCLK1 cells to increasing concentrations of sunitinib and sorafenib for 48 hr and performed an MTT assay. Caki-2-dsRed-DCLK1 cells resisted sunitinib compared to controls at most doses (ANOVA $p < 0.05$). In contrast, although there was resistance to sorafenib at lower doses, the effect was insignificant (Fig. 5a). To test this effect further, we repeated spheroid assays following pretreatment with sunitinib. Under these conditions, Caki-2-dsRed-DCLK1 cells maintained clonogenic ability compared to control cells (Fig. 5b, Supporting Information Fig. 7a). In addition to receptor tyrosine kinase inhibitors (RTKIs), the FDA has approved mTOR inhibitors everolimus and temsirolimus for RCC. Repeating the MTT assays above, we found that Caki-2-dsRed-DCLK1 cells resisted both mTOR inhibitors (Supporting Information Fig. 6d). These findings suggest that DCLK1 expression is an important factor in RCC drug resistance.

To test whether DCLK1-targeted therapies can overcome resistance, we transfected Caki-2 and ACHN cells with DCLK1-targeted siRNA, confirmed DCLK1 knockdown by western blot (Fig. 5c), and treated with varying doses of RTKIs. DCLK1 knockdown sensitized both cell lines to RTKIs at varying doses (Fig. 5d). Given these findings, spheroid assays with sunitinib pretreatment were repeated in Caki-2 cells following DCLK1 knockdown. DCLK1 siRNA in combination with sunitinib caused a 2.5 to fourfold decrease in spheroid formation compared to controls treated with sunitinib and scrambled siRNA (Fig. 5e).

Anti-proliferative activity is a secondary mechanism of RTKI anti-tumor activity,^{39,40} and some reports suggest that this activity may be overcome through EMT induction, TSC resistance or other mechanisms.⁴⁰⁻⁴² Other findings show TSCs which resist this activity can undergo endothelial differentiation in which they become susceptible,⁴³ or that TSCs become susceptible at increased dose.⁴⁴ To determine whether DCLK1 may have a role in angiogenic/vasculogenic activity that RTKIs target, we performed a surrogate assay using HUVEC endothelial cells plated in growth factor reduced matrigel with or without 200 nM of sunitinib and with or without supportive ACHN cells pretransfected with scrambled or DCLK1-specific siRNA for 48 hr plated in 0.4 μm transwells. In the presence of tumor cells, HUVECs were able to form tubule structures when treated with sunitinib, but this activity was strongly reduced in HUVECs plated with ACHN cells that were pretreated with DCLK1 siRNA compared to scrambled siRNA as measured by total tubule length (Figs. 5f and 5g) and mean tubule length (Supporting Information Figs. 5b and 5d). Together with findings of

cell growth inhibition in combination with RTK inhibitors, these findings support targeting DCLK1 synergistically with RTKIs in RCC.

Immune-checkpoint is associated with DCLK1-long in RCC patient tumors

PD-L1 is an immune checkpoint membrane marker expressed on various tumors, including RCC.⁴⁵ It negatively regulates the immune response by binding to PD-1 on T-cells leading to apoptosis and allowing escape from tumor cytolysis induced by activated T-cells.⁴⁶ Moreover, both PD-L1 and CTLA4 are targets of novel therapies that may extend RCC survival.³² Importantly, PD-L1 is associated with EMT^{34–38} and a likely mechanism by which TSCs avoid immune-mediated destruction in an EMT environment. While RCC often resists therapy, studies focusing on immunotherapies, including the PD-L1/PD-1 interaction have shown promising results.^{47,48} Considering the KEGG analysis demonstrating that the majority of pathways enriched in DCLK1+ RCC are immune-related (Supporting Information Table I) and expression analysis indicating that DCLK1-long- α leads to increased expression of PD-L1 and CTLA4 proteins in RCC (Fig. 3a), we set out to determine if DCLK1-long and PD-L1 are coexpressed in RCC. Immunohistochemistry results demonstrated that PD-L1 was upregulated stage-wise in RCC (Fig. 6a). Moreover, tumors with membrane PD-L1 demonstrated higher DCLK1-long expression (Fig. 6b). These findings demonstrate coexpression of DCLK1 and membrane PD-L1, which is the functional form of this marker and further illustrate the potential therapeutic value of DCLK1 in RCC.

DCLK1-long monoclonal antibody therapy inhibits renal cancer tumorigenesis *in vivo*

Given DCLK1-long's extracellular domain (Supporting Information Fig. 7b), we hypothesized that monoclonal antibodies (mAbs) may be suitable to target DCLK1+ cells in cancer. We obtained a DCLK1-long targeted mAb (CBT-15) and performed ELISA to test its affinity for DCLK1-long (Supporting Information Fig. 7c). CBT-15 demonstrated an EC₅₀ of approximately 1.02 nM for DCLK1-long compared to no specific binding for DCLK1-short, and could detect DCLK1-long- β by immunoblot (Supporting Information Figs. 7c and 7d). Cells treated with CBT-15 demonstrated no toxicity at up to 200 μ g/mL (data not shown) and no significant changes in DCLK1-long expression. However, CBT-15 did appear to modestly downregulate PD-L1 in Caki-2 cells (Supporting Information Fig. 7d). Considering the lack of toxicity observed with CBT-15 *in vitro*, we repeated the experiment with the addition of peripheral blood monocytes (PBMCs). In combination, CBT-15 increased cell apoptosis as measured by caspase-3/7 activity suggesting antibody-dependent cell-mediated cytotoxicity (ADCC) (Fig. 6c). Moreover, CBT-15 was able to bind CD16, which mediates ADCC, in an antigen-dependent fashion (Supporting Information Fig. 7e).

To measure CBT-15's *in vivo* efficacy in RCC, we established ACHN xenografts in athymic nude mice. At an average tumor volume of 100 mm³, the animals were injected i.p. with CBT-15 or isotype at 25 mg/kg biweekly ($n = 6$) and tumor volume was measured triweekly. CBT-15 inhibited ACHN xenograft growth compared to isotype (Fig. 6d, $p < 0.03$). This was confirmed by measuring excised tumors (Figs. 6e and 6g, $p < 0.001$, $p < 0.01$). Additionally, immunostaining showed high DCLK1 expression in isotype-treated ACHN xenograft tumors

which decreased appreciably following CBT-15 (Fig. 6h). These findings demonstrate *in vivo* efficacy of DCLK1-targeted mAb against RCC. Given RCC's potent resistance to therapy, DCLK1-targeted agents should be further investigated in this context. However, further research to determine the mechanisms mediated by extracellular DCLK1 will be needed.

Discussion

RCC is characterized by slow-growth, hypoxia and drug-resistance consistent with the presence of TSCs.^{28,49} Previous findings demonstrate that DCLK1 is epigenetically dysregulated and overexpressed in RCC. Moreover, downregulation of DCLK1 in RCC decreases hallmarks of tumorigenesis and metastasis.¹⁶ In this study, we found that DCLK1 alternative splice variants (DCLK1 ASVs) were enriched with RCC stem cell markers ALDH, CXCR4 and CD44. Moreover, DCLK1 ASVs were associated with recurrence. Because DCLK1 marks TSCs, high expression is likely more relevant during early disease before a variety of progeny have populated the tumor bulk. Predictably, patients with high DCLK1 ASVs during low-grade or early stage disease had reduced overall survival. These data together with DCLK1's tumor-specific overexpression suggest that it may mark RCC TSCs in an isoform-specific fashion and have potential as a biomarker.

To expand on our patient data, we overexpressed DCLK1 ASV (Isoform 2) in RCC cells and assessed TSC characteristics. Overexpression of DCLK1-ASV in RCC induced ALDH and HIF1A, spheroid formation and RTKI resistance. Conversely, siRNA-mediated downregulation of DCLK1 sensitized RCC to RTKIs and mTOR inhibitors. These findings in combination with our findings in patient tumors, FACS studies demonstrating DCLK1/ALDH double-positive subpopulations, ALDH-positive DCLK1-overexpressing spheroids and our previous work¹⁶ suggest that DCLK1 is a functional target that is coexpressed with ALDH in RCC TSCs.

Targeting DCLK1 has proven to be effective *in vivo* against gastrointestinal cancer.^{13,26,27} Pancreatic cancer shares TSC markers with RCC including ALDH, CXCR4, CD44 and others.⁵⁰ Moreover, as we demonstrate here in RCC, DCLK1+ cells are also enriched with the ALDH TSC marker in pancreatic cancer.¹² Additionally, given the patient and functional data supporting a role for DCLK1 in RCC drug resistance, clonogenicity, recurrence and survival, we assessed the potential for DCLK1-targeted agents against *in vivo* tumorigenesis. The most basic form of specific targeted therapy with demonstrated success in patients are monoclonal antibodies (mAbs). Generally, for a mAb to be effective in patients its target must be extracellular and relatively restricted to the tumor. DCLK1 contains an extracellular domain^{14,15} and its expression in normal renal tissue is restricted but overexpressed in RCC.¹⁶ To assess DCLK1-targeted mAb therapy we obtained mAb raised against the DCLK1 extracellular domain (CBT-15). We found that CBT-15 was nontoxic, but could induce apoptosis in the presence of immune cells. Importantly, systemic biweekly CBT-15 was well-tolerated and reduced tumorigenesis in RCC xenografts. To our knowledge, this is the first peer-reviewed report of a therapeutic DCLK1 mAb *in vitro* and *in vivo*, and the first to demonstrate specific targeting of DCLK1 in RCC *in vivo*.

Overall, the findings presented here suggest DCLK1 is a potential renal TSC marker and that assessing DCLK1 antibodies or other DCLK1-detection reagents as RCC biomarkers is warranted. Additionally, they add to the literature demonstrating unique functions for DCLK1 isoforms and highlight the importance of studying these individually. Future studies should focus on determining if normal DCLK1+ kidney cells may serve as tumor-initiating cells in animal models, elucidating DCLK1's role in regulating immune checkpoint, and assessing anti-DCLK1 therapies in orthotopic RCC models.

Supplementary Material

Refer to Web version on PubMed Central for supplementary material.

Acknowledgements

We would like to thank Sheeja Aravindan and Louisa Williams of the Stephenson Cancer Center Tissue Pathology Core Lab for assistance with immunohistochemistry of xenograft tissues. We would also like to thank Edwin Bannerman-Menson and Sripathi Sureban of COARE for providing CBT-15 mAB for testing.

Grant sponsor: National Cancer Institute; **Grant number:** 2-R44CA174025-02

REFERENCES

1. Siegel RL, Miller KD, Jemal A. Cancer statistics, 2015. *CA Cancer J Clin*2015;65:5–29. [PubMed: 25559415]
2. Koul H, Huh JS, Rove KO, et al. Molecular aspects of renal cell carcinoma: a review. *Am J Cancer Res*2011;1:240–54. [PubMed: 21969126]
3. Myszczyzyn A, Czarnecka AM, Matak D, et al. The role of hypoxia and cancer stem cells in renal cell carcinoma pathogenesis. *Stem Cell Rev*2015;11:919–43.
4. Bussolati B, Dekel B, Azzarone B, et al. Human renal cancer stem cells. *Cancer Lett*2013;338: 141–6. [PubMed: 22587951]
5. Hsieh JJ, Purdue MP, Signoretti S, et al. Renal cell carcinoma. *Nat Rev Dis Primers*2017;3: 17009. [PubMed: 28276433]
6. Axelson H, Johansson ME. Renal stem cells and their implications for kidney cancer. *Semin Cancer Biol*2013;23:56–61. [PubMed: 22766133]
7. Marusyk A, Polyak K. Tumor heterogeneity: causes and consequences. *Biochim Biophys Acta*2010;1805:105–17. [PubMed: 19931353]
8. Krabbe LM, Westerman ME, Bagrodia A, et al. Dysregulation of beta-catenin is an independent predictor of oncological outcomes in patients with clear cell renal cell carcinoma. *J Urol*2014; 191:1671–7. [PubMed: 24291548]
9. Harada K, Miyake H, Kusuda Y, et al. Expression of epithelial-mesenchymal transition markers in renal cell carcinoma: impact on prognostic outcomes in patients undergoing radical nephrectomy. *BJU Int*2012;110:E1131–7. [PubMed: 22712620]
10. Philip B, Ito K, Moreno-Sanchez R, et al. HIF expression and the role of hypoxic microenvironments within primary tumours as protective sites driving cancer stem cell renewal and metastatic progression. *Carcinogenesis*2013;34:1699–707. [PubMed: 23740838]
11. Nakanishi Y, Seno H, Fukuoka A, et al. Dcl1 distinguishes between tumor and normal stem cells in the intestine. *Nat Genet*2013;45:98–103. [PubMed: 23202126]
12. Bailey JM, Alsina J, Rasheed ZA, et al. DCLK1 marks a morphologically distinct subpopulation of cells with stem cell properties in preinvasive pancreatic cancer. *Gastroenterology*2014;146:245–56. [PubMed: 24096005]
13. Weygant N, Qu D, Berry WL, et al. Small molecule kinase inhibitor LRRK2-IN-1 demonstrates potent activity against colorectal and pancreatic cancer through inhibition of doublecortin-like kinase 1. *Mol Cancer*2014;13:103. [PubMed: 24885928]

14. Wibowo A, Peters EC, Hsieh-Wilson LC. Photoactivatable glycopolymers for the proteome-wide identification of fucose- $\alpha(1-2)$ -galactose binding proteins. *J Am Chem Soc*2014;136:9528–31. [PubMed: 24937314]
15. May R, Sureban SM, Hoang N, et al. Doublecortin and CaM kinase-like-1 and leucine-rich-repeat-containing G-protein-coupled receptor mark quiescent and cycling intestinal stem cells, respectively. *Stem Cells*2009;27:2571–9. [PubMed: 19676123]
16. Weygant N, Qu D, May R, et al. DCLK1 is a broadly dysregulated target against epithelial-mesenchymal transition, focal adhesion, and stemness in clear cell renal carcinoma. *Oncotarget*2015;6:2193–205. [PubMed: 25605241]
17. Weygant N, Qu D, May R, et al. Abstract 577: systemic delivery of CBT-15G DCLK1-targeted monoclonal antibody dramatically decreases tumorigenesis in a xenograft model of pancreatic cancer. *Cancer Res*2016;76:577.
18. Wang J, Vasaikar S, Shi Z, et al. WebGestalt 2017: a more comprehensive, powerful, flexible and interactive gene set enrichment analysis toolkit. *Nucleic Acids Res*2017;45:W130–7. [PubMed: 28472511]
19. Yang Y, Faraggi E, Zhao H, et al. Improving protein fold recognition and template-based modeling by employing probabilistic-based matching between predicted one-dimensional structural properties of query and corresponding native properties of templates. *Bioinformatics*2011;27:2076–82. [PubMed: 21666270]
20. Corro C, Moch H. Biomarker discovery for renal cancer stem cells. *J Pathol Clin Res*2018;4:3–18. [PubMed: 29416873]
21. Bankhead P, Loughrey MB, Fernandez JA, et al. QuPath: open source software for digital pathology image analysis. *Sci Rep*2017;7:16878. [PubMed: 29203879]
22. Vedeld HM, Skotheim RI, Lothe RA, et al. The recently suggested intestinal cancer stem cell marker is an epigenetic biomarker for colorectal cancer. *Epigenetics*2014;9:346. [PubMed: 24384857]
23. Burgess HA, Reiner O. Alternative splice variants of doublecortin-like kinase are differentially expressed and have different kinase activities. *J Biol Chem*2002;277:17696–705. [PubMed: 11884394]
24. Kadletz L, Thurnher D, Wiebringhaus R, et al. Role of cancer stem-cell marker doublecortin-like kinase 1 in head and neck squamous cell carcinoma. *Oral Oncol*2017;67:109–18. [PubMed: 28351564]
25. Weygant N, Ge Y, Qu D, et al. Survival of patients with gastrointestinal cancers can be predicted by a surrogate microRNA signature for cancer stem-like cells marked by DCLK1 kinase. *Cancer Res*2016;76:4090–9. [PubMed: 27287716]
26. Westphalen CB, Takemoto Y, Tanaka T, et al. Dclk1 defines quiescent pancreatic progenitors that promote injury-induced regeneration and tumorigenesis. *Cell Stem Cell*2016;18:441–55. [PubMed: 27058937]
27. Westphalen CB, Asfaha S, Hayakawa Y, et al. Long-lived intestinal tuft cells serve as colon cancer-initiating cells. *J Clin Invest*2014;124: 1283–95. [PubMed: 24487592]
28. Wang K, Chen X, Zhan Y, et al. Increased expression of ALDH1A1 protein is associated with poor prognosis in clear cell renal cell carcinoma. *Med Oncol*2013;30:574. [PubMed: 23585015]
29. Chen D, Gassenmaier M, Maruschke M, et al. Expression and prognostic significance of a comprehensive epithelial-mesenchymal transition gene set in renal cell carcinoma. *J Urol*2014;191: 479–86. [PubMed: 24012533]
30. Li G, Badin G, Zhao A, et al. Prognostic value of CXCR4 expression in patients with clear cell renal cell carcinoma. *Histol Histopathol*2013;28: 1217–22. [PubMed: 23609324]
31. Mikami S, Mizuno R, Kosaka T, et al. Expression of TNF- α and CD44 is implicated in poor prognosis, cancer cell invasion, metastasis and resistance to the sunitinib treatment in clear cell renal cell carcinomas. *Int J Cancer*2015;136: 1504–14. [PubMed: 25123505]
32. Motzer RJ, Escudier B, McDermott DF, et al. Nivolumab versus everolimus in advanced renal cell carcinoma. *N Engl J Med*2015;373:1803–13. [PubMed: 26406148]

33. Yang JC, Hughes M, Kammula U, et al. Ipilimumab (anti-CTLA4 antibody) causes regression of metastatic renal cell cancer associated with enteritis and hypophysitis. *J Immunother* 2007;30:825–30. [PubMed: 18049334]
34. Noman MZ, Janji B, Abdou A, et al. The immune checkpoint ligand PD-L1 is upregulated in EMT-activated human breast cancer cells by a mechanism involving ZEB-1 and miR-200. *Oncoimmunology* 2017;6:e1263412. [PubMed: 28197390]
35. Tsutsumi S, Saeki H, Nakashima Y, et al. PD-L1 expression at tumor invasive front is associated with EMT and poor prognosis in esophageal squamous cell carcinoma. *Cancer Sci.* 2017;108:1119–27. [PubMed: 28294486]
36. Kim S, Koh J, Kim MY, et al. PD-L1 expression is associated with epithelial-to-mesenchymal transition in adenocarcinoma of the lung. *Hum Pathol* 2016;58:7–14. [PubMed: 27473266]
37. Alsuliman A, Colak D, Al-Harazi O, et al. Bidirectional crosstalk between PD-L1 expression and epithelial to mesenchymal transition: significance in claudin-low breast cancer cells. *Mol Cancer* 2015;14:149. [PubMed: 26245467]
38. Wang Y, Wang H, Zhao Q, et al. PD-L1 induces epithelial-to-mesenchymal transition via activating SREBP-1c in renal cell carcinoma. *Med Oncol* 2015;32:212. [PubMed: 26141060]
39. van der Mijn JC, Broxterman HJ, Knol JC, et al. Sunitinib activates Axl signaling in renal cell cancer. *Int J Cancer* 2016;138:3002–10. [PubMed: 26815723]
40. Sakai I, Miyake H, Fujisawa M. Acquired resistance to sunitinib in human renal cell carcinoma cells is mediated by constitutive activation of signal transduction pathways associated with tumour cell proliferation. *BJU Int* 2013;112:E211–20. [PubMed: 23305097]
41. Zhou L, Liu XD, Sun M, et al. Targeting MET and AXL overcomes resistance to sunitinib therapy in renal cell carcinoma. *Oncogene* 2016;35:2687–97. [PubMed: 26364599]
42. Chinchar E, Makey KL, Gibson J, et al. Sunitinib significantly suppresses the proliferation, migration, apoptosis resistance, tumor angiogenesis and growth of triple-negative breast cancers but increases breast cancer stem cells. *Vasc Cell* 2014; 6:12. [PubMed: 24914410]
43. Brossa A, Grange C, Mancuso L, et al. Sunitinib but not VEGF blockade inhibits cancer stem cell endothelial differentiation. *Oncotarget* 2015;6:11295–309. [PubMed: 25948774]
44. Czarnicka AM, Solarek W, Kornakiewicz A, et al. Tyrosine kinase inhibitors target cancer stem cells in renal cell cancer. *Oncol Rep* 2016;35:1433–42. [PubMed: 26708631]
45. Afreen S, Dermime S. The immunoinhibitory B7-H1 molecule as a potential target in cancer: killing many birds with one stone. *Hematol Oncol Stem Cell Ther* 2014;7:1–17. [PubMed: 24398144]
46. Blank C, Gajewski TF, Mackensen A. Interaction of PD-L1 on tumor cells with PD-1 on tumor-specific T cells as a mechanism of immune evasion: implications for tumor immunotherapy. *Cancer Immunol Immunother* 2005;54:307–14. [PubMed: 15599732]
47. Pardoll DM. The blockade of immune checkpoints in cancer immunotherapy. *Nat Rev Cancer* 2012;12:252–64. [PubMed: 22437870]
48. Brahmer JR, Tykodi SS, Chow LQ, et al. Safety and activity of anti-PD-L1 antibody in patients with advanced cancer. *N Engl J Med* 2012;366:2455–65. [PubMed: 22658128]
49. Ueda K, Ogasawara S, Akiba J, et al. Aldehyde dehydrogenase 1 identifies cells with cancer stem cell-like properties in a human renal cell carcinoma cell line. *PLoS One* 2013;8:e75463. [PubMed: 24116047]
50. Vaz AP, Ponnusamy MP, Seshacharyulu P, et al. Concise review on the current understanding of pancreatic cancer stem cells. *J Cancer Stem Cell Res* 2014;2:1.

What's new?

Doublecortin-like kinase 1 (DCLK1) is a validated marker for cancer stem cells in the gastrointestinal tract but its role in other cancers is unclear. Here, the authors demonstrate that specific DCLK1 alternative splice variants are overexpressed in renal cell cancer and drive self-renewal and resistance to standard of care chemotherapies in cell culture coexpression experiments. As targeting the extracellular domain of DCLK1 variants by a monoclonal antibody (CBT-15) results in strong inhibition of tumor growth *in vivo*, these findings may open new therapeutic options for patients afflicted with this commonly intractable cancer.

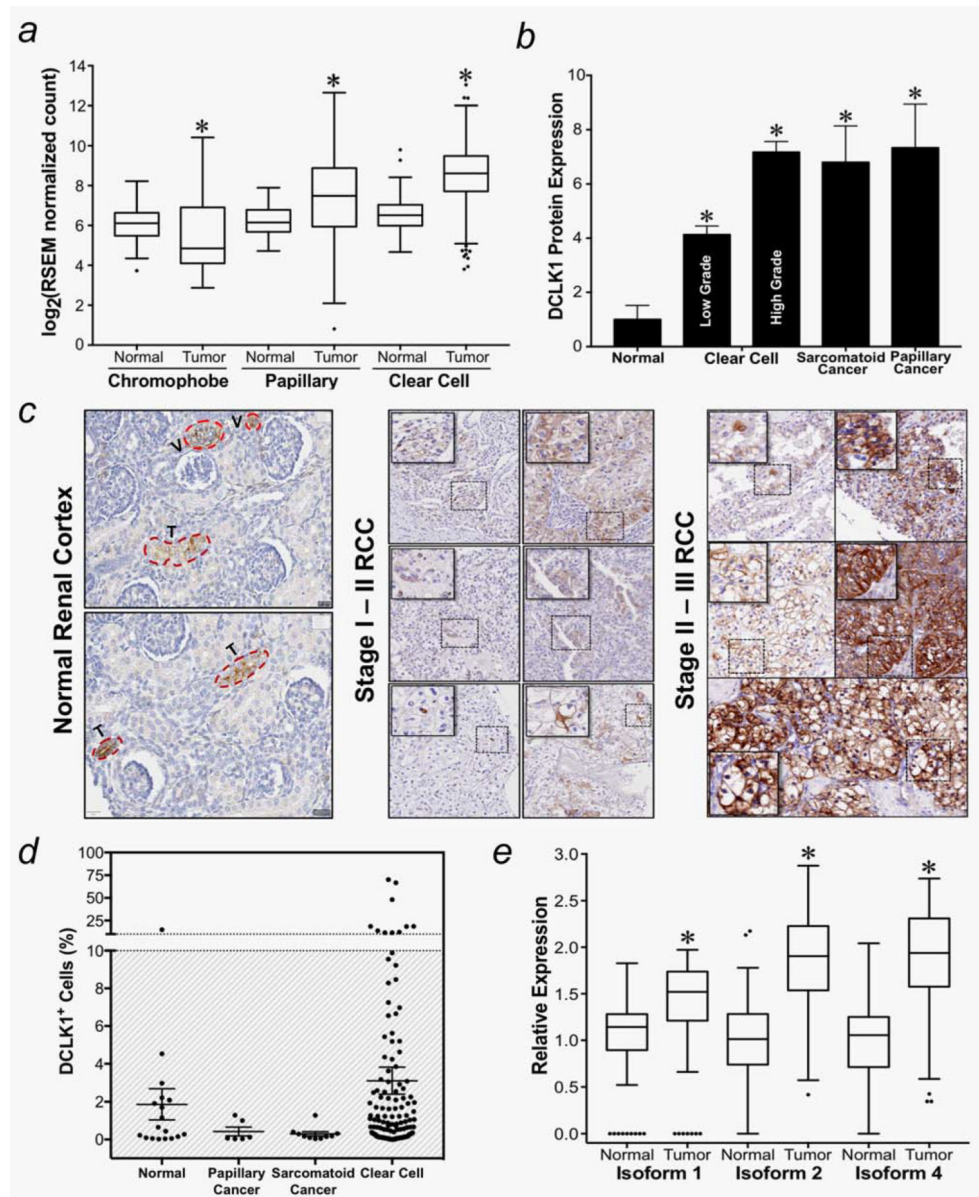


Figure 1. DCLK1 is overexpressed in renal cancer subtypes. (a) DCLK1 mRNA is overexpressed in papillary ($n = 290$) and clear cell ($n = 533$) renal cancers, but downregulated in chromophobe cancer ($n = 66$, $*p < 0.0001$) in the TCGA PANCAN dataset. (b) Immunohistochemistry reveals that DCLK1 is overexpressed in clear cell ($n = 165$), papillary ($n = 6$) and sarcomatoid ($n = 10$) renal cancer compared to normal tissue ($*p < 0.002$). (c) Representative images of DCLK1 expression in normal and stages I–III clear cell RCC. (d) DCLK1+ cells represent a minority of RCC cell populations and occur in the greatest numbers in clear cell RCC. (e) DCLK1 alternative transcripts (Isoforms 2 and 4) demonstrate greater upregulation compared to normal tissue than canonical DCLK1 Isoform 1 transcript ($*p < 0.0001$ for all).

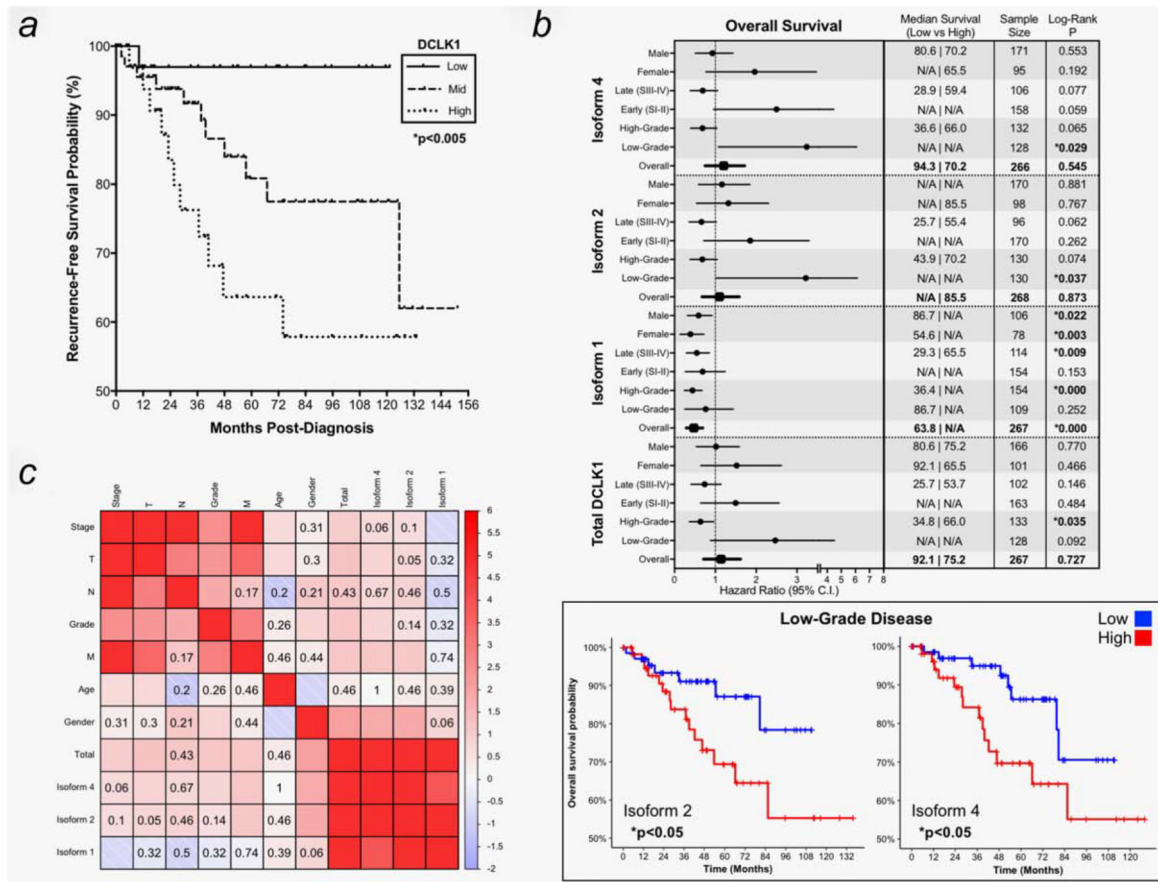


Figure 2. DCLK1 alternative transcript expression predicts RCC recurrence and survival. (a) Increased levels of DCLK1 gene expression predict significantly decreased recurrence-free survival. Low expression of DCLK1 predicts a <4% probability of recurrence for RCC patients over the course of >11 years. (b) Subgroup analysis demonstrates that DCLK1 alternative transcripts (Isoforms 2 and 4) predict significantly decreased overall survival when they are expressed at high levels in low-grade disease ($p < 0.05$) while expression of canonical Isoform 1 predicts increased survival ($p < 0.001$). (c) Correlation analysis demonstrating relationship between DCLK1 gene expression and clinical factors. Blocks without numbers indicate a significance level of $p < 0.05$.

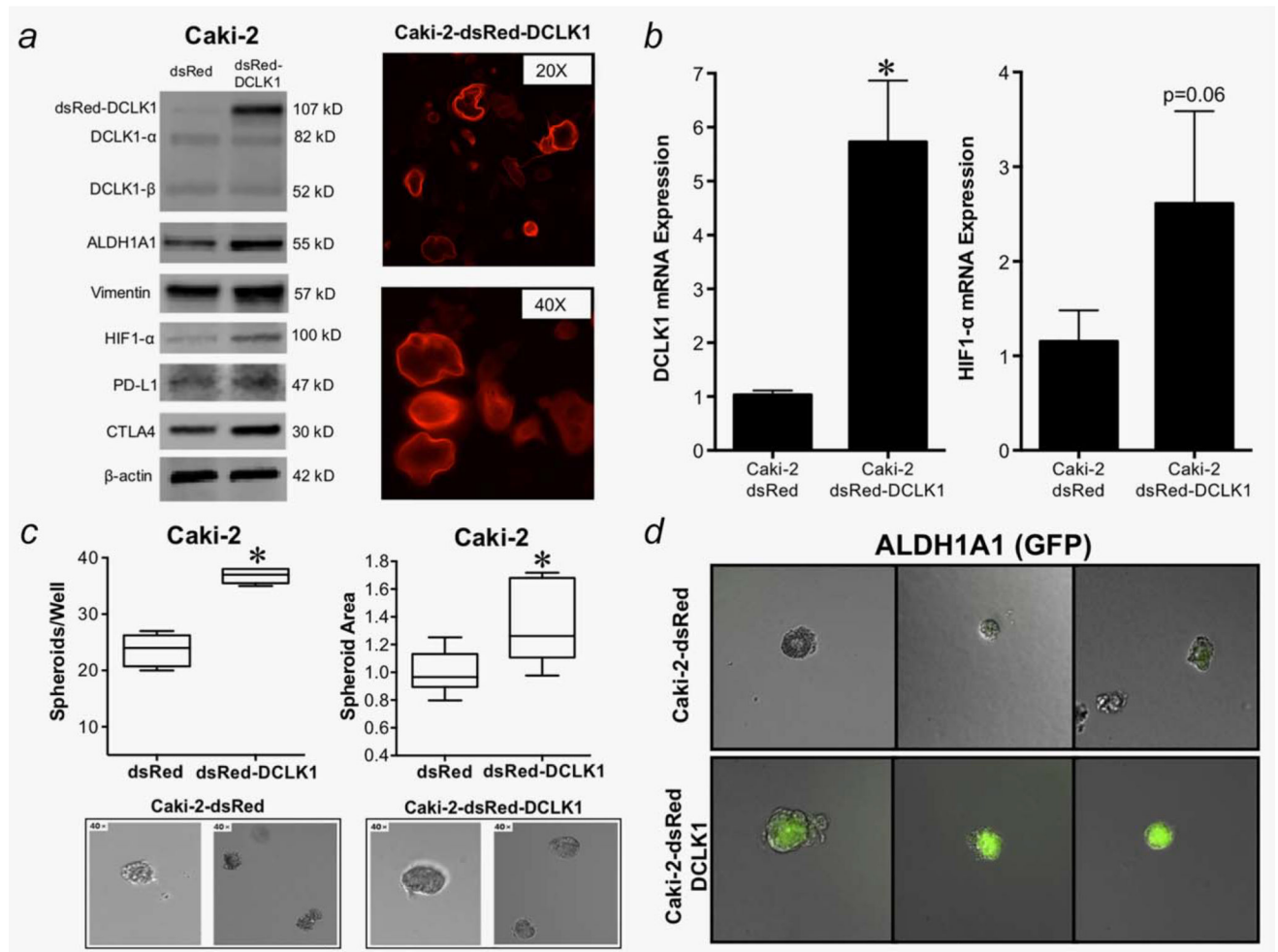


Figure 3.

Overexpression of DCLK1 alternative transcript (Isoform 2) drives expression of RCC stem cell markers and enhances self-renewal ability. (a, b) DCLK1-overexpressing Caki-2 RCC cells (Caki-2-dsRed-DCLK1) demonstrate a dramatic upregulation in DCLK1 protein and mRNA expression ($*p < 0.05$). Fluorescence imaging of the dsRed-tagged DCLK1 overexpressing cells demonstrate a primarily microtubule/cytoskeletal localization for this isoform (Isoform 2; DCLK1-long- α) in this cell line. Moreover, DCLK1 overexpression increases expression of EMT/cancer stem cell marker proteins ALDH1A1, HIF-1 α and vimentin as well as immune-checkpoint markers PD-L1 and CTLA4. (c) In matrigel self-renewal assays, Caki-2-dsRed-DCLK1 cells form larger and greater numbers of spheroids compared to vector control cells ($*p < 0.05$). (d) Caki-2-dsRed-DCLK1 spheroids demonstrate increased ALDH protein expression compared to vector control cells, suggesting that DCLK1 alternative transcript and ALDH may cooperate to drive self-renewal.

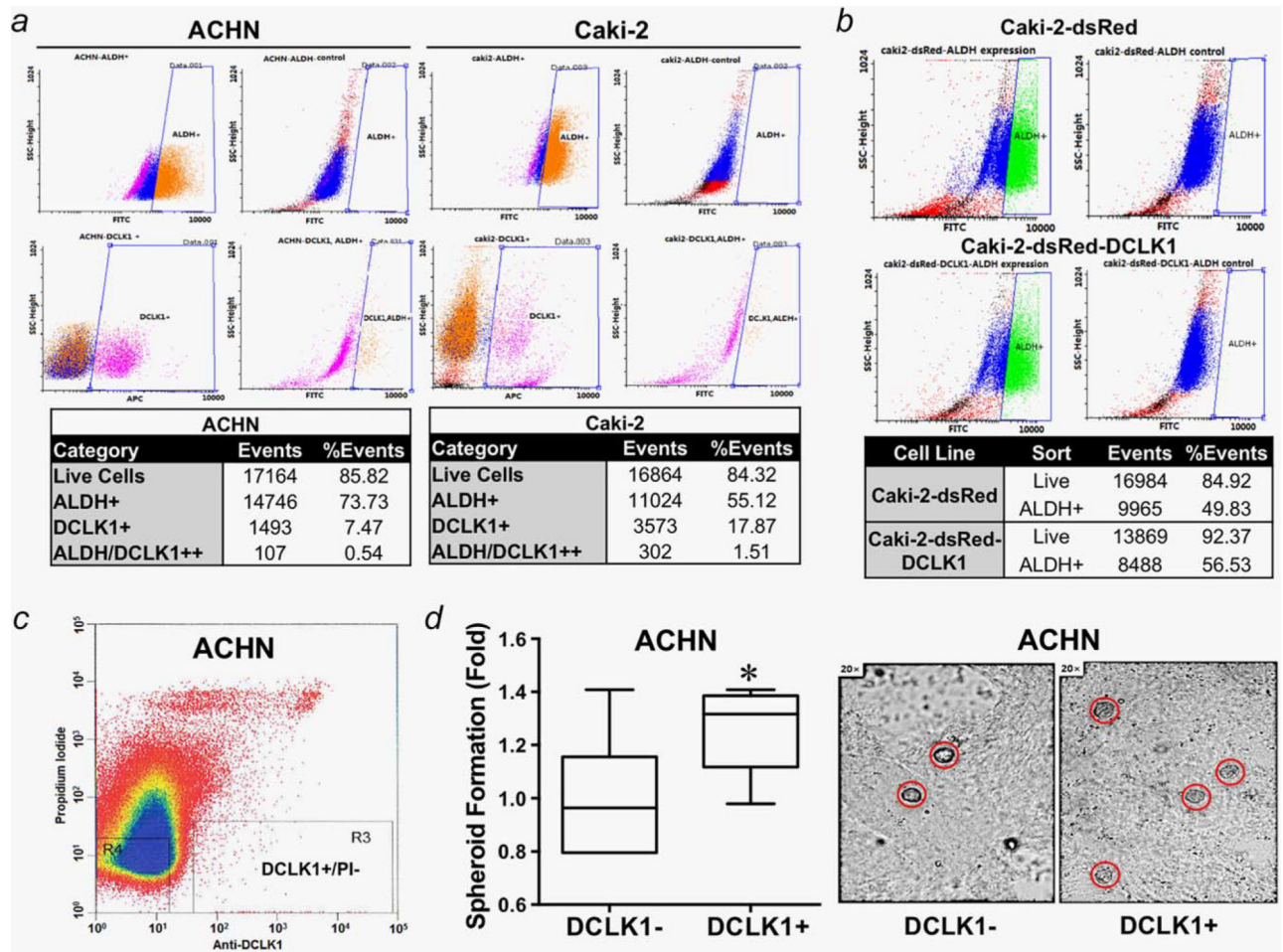


Figure 4.

DCLK1 alternative transcripts are coexpressed with ALDH in a small subpopulation of RCC cells and their expression leads to increased self-renewal capacity *in vitro*. (a) FACS results demonstrate the existence of a 0.54% and 1.51% subpopulation of ALDH/DCLK1-alternative transcript positive cells in ACHN and Caki-2 RCC cell lines. (b) Overexpression of DCLK1 alternative transcript (Isoform 2) in Caki-2 cells (Caki-2-dsRed-DCLK1) leads to a 7% increase in the number of ALDH1 cells. (c) DCLK1+ cells can be sorted under nonpermeabilizing conditions from the ACHN cell line by FACS using antibody targeting the extracellular domain. (d) Sorted ACHN-DCLK1+ cells demonstrate a >25% increase in spheroid formation compared to ACHN-DCLK1- cells (* $p < 0.05$). [Color figure can be viewed at wileyonlinelibrary.com]

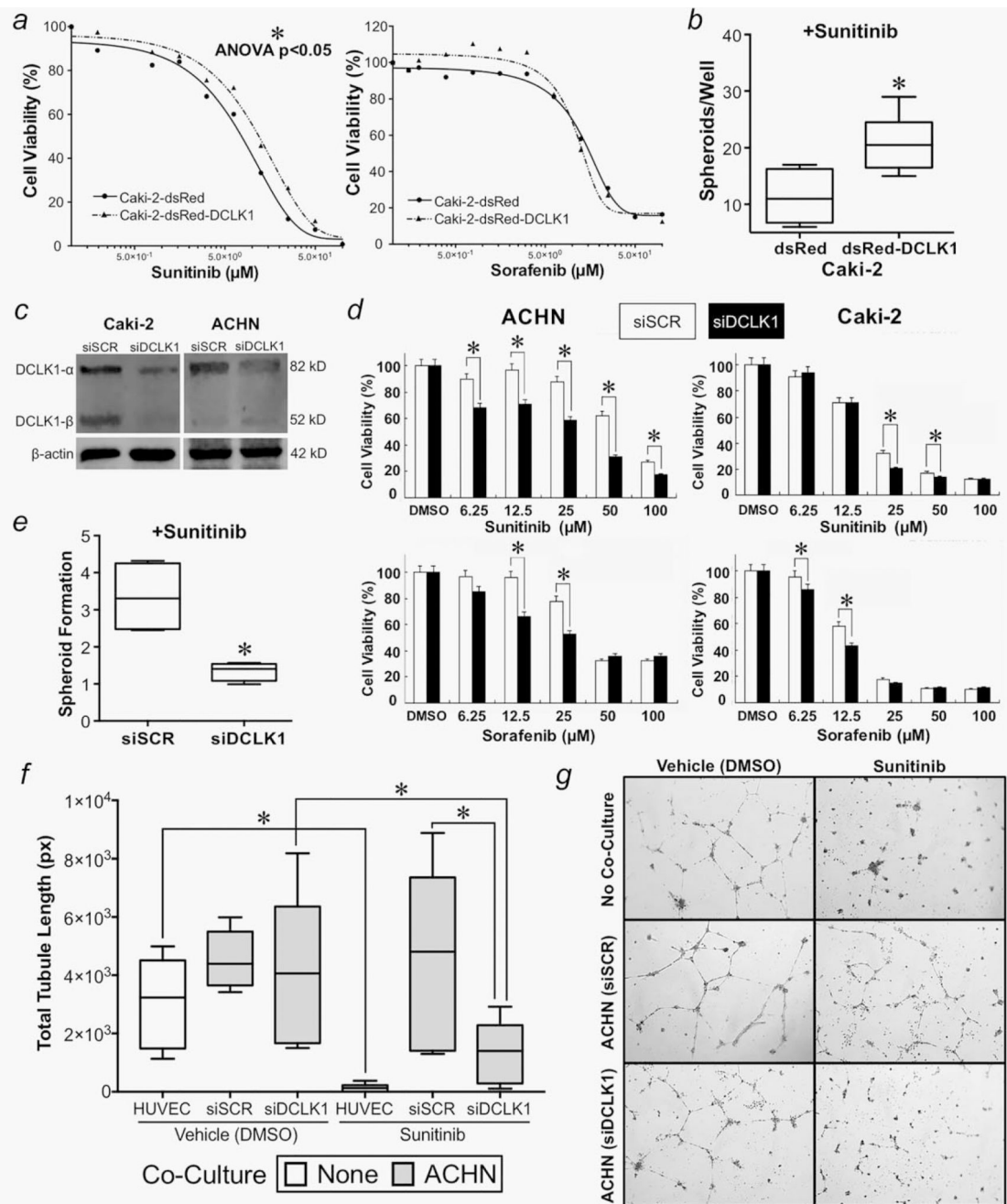
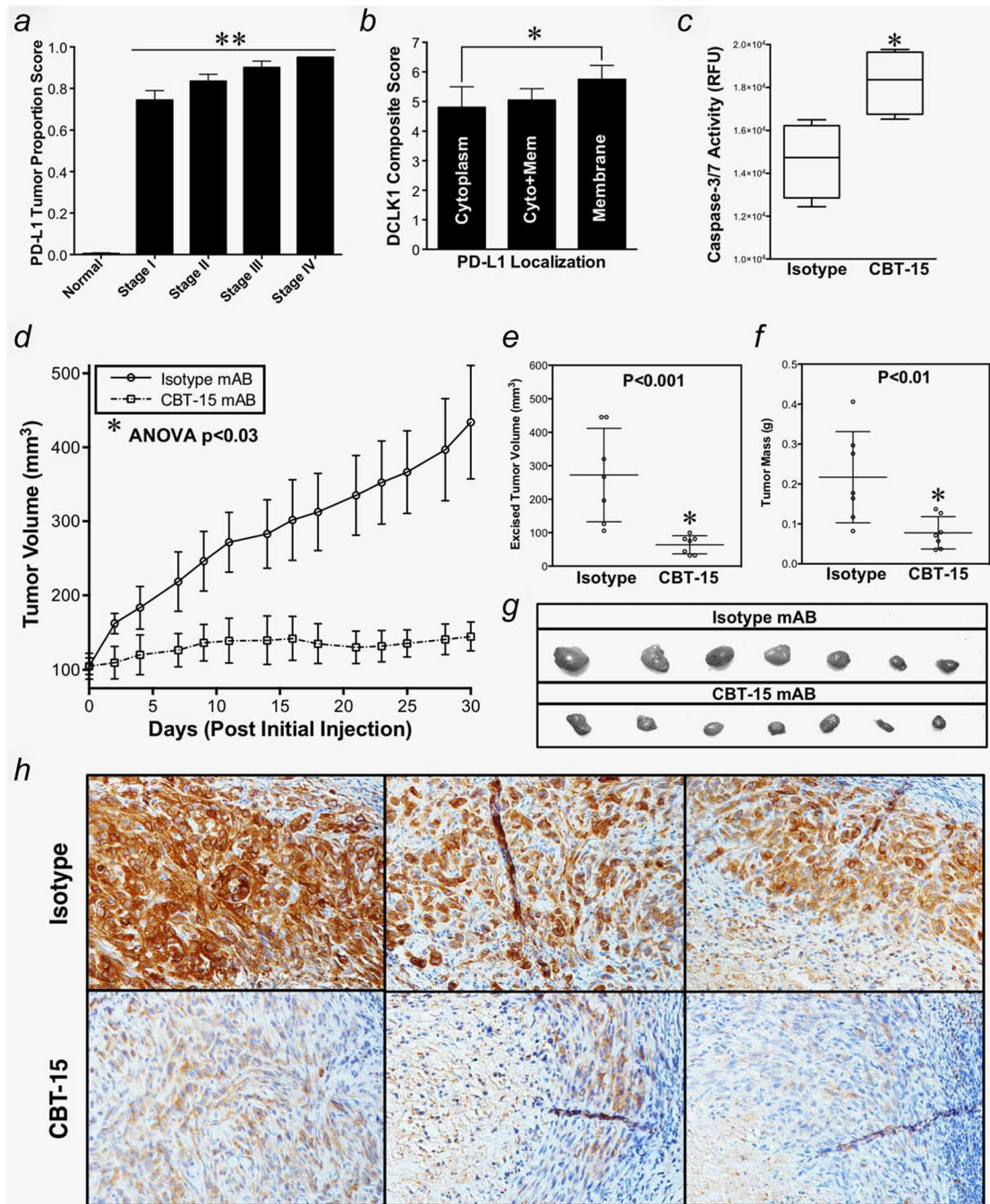


Figure 5. Overexpression of DCLK1 alternative transcript (Isoform 2) enhances drug resistance and self-renewal ability. In contrast, targeted downregulation of DCLK1 expression sensitizes RCC cells to receptor tyrosine kinase inhibitors. (*a, b*) Caki-2-dsRed-DCLK1 cells resist sunitinib in MTT and matrigel self-renewal assays ($*p < 0.05$). However, Caki-2-dsRed-DCLK1 cells do not demonstrate comparable resistance to sorafenib by MTT assay. (*c*) Transfection of Caki-2 and ACHN RCC cells with 25 nM siDCLK1 for 72 hr leads to downregulation of DCLK1 alternative transcript protein expression of the 52 kDa (Isoform

4) and 82 kDa (Isoform 2) forms. (d) siDCLK1 and sunitinib coadministration to Caki-2 cells leads to significantly impaired self-renewal in matrigel ($*p < 0.01$). (e) Targeted downregulation of DCLK1 in Caki-2 and ACHN cell lines results in significant sensitization to FDA-approved receptor tyrosine kinase inhibitors sunitinib and sorafenib. (f, g) HUVEC cells are capable of forming tubes following 200 nM sunitinib in the presence of ACHN RCC cells, but total tubule length is significantly decreased in HUVECs supported by ACHN RCC cells that have been pretreated with DCLK1 siRNA compared to scrambled controls ($p < 0.05$).

**Figure 6.**

DCLK1 alternative transcript expression of RCC cells is associated with membrane PD-L1. CBT-15 DCLK1-targeted mAB treatment sensitizes ACHN RCC cell line to ADCC in vitro and results in powerful inhibition of ACHN tumor xenograft growth in vivo. (a) PD-L1 is strongly upregulated in RCC compared to normal tissue (** $p < 0.005$) in an apparent stage-dependent fashion. (b) Tumors with membranelocalized PD-L1 demonstrated significantly higher DCLK1 expression levels compared to patients with cytoplasmic PD-L1 (* $p < 0.05$). (c) CBT-15 DCLK1-targeted mAB treatment sensitizes ACHN RCC cells to

apparent immune-mediated apoptosis as measured by caspase-3/7 activity (* $p < 0.02$). (*a-g*) Biweekly injections of novel CBT-15 mAB significantly impairs ACHN tumor xenograft growth ($p < 0.03$) as confirmed by (*e*) decreased excised tumor volume and (*f*) decreased excised tumor mass (* $p < 0.01$ for both). (*h*) Immunohistochemical staining demonstrating decreased DCLK1 in CBT-15 treated tumors compared to controls.